PHYSICAL REVIEW B **82**, 113106 (2010)

Exciton-exciton annihilation in organic polariton microcavities

G. M. Akselrod,[1] Y. R. Tischler,[2,*] E. R. Young,[3] D. G. Nocera,[3] and V. Bulovic[2]
[1]*Department of Physics, Massachusetts Institute of Technology, Cambridge, Massachusetts 02139, USA*
[2]*Department of Electrical Engineering, Massachusetts Institute of Technology, Cambridge, Massachusetts 02139, USA*
[3]*Department of Chemistry, Massachusetts Institute of Technology, Cambridge, Massachusetts 02139, USA*

(Received 30 May 2010; revised manuscript received 24 August 2010; published 27 September 2010)

We investigate the incoherent diffusion of excitons in thin films (5.1 ± 0.1 nm thick) of a highly absorbing J-aggregated cyanine dye material (10^6 cm^{-1} absorption constant) as the excitonic component of a polariton microcavity. Under high-intensity pulsed laser excitation, the J-aggregated molecular films exhibit significant exciton-exciton annihilation, indicating a large exciton diffusion radius of more than 100 nm. When the material is strongly coupled to a cavity, the polaritonic structure also shows exciton-exciton annihilation, which is a competing process against the establishment of a threshold population of polaritons needed for polariton lasing. This study suggests that exciton-exciton annihilation is a loss process which can significantly increase the lasing threshold in polariton microcavities.

DOI: 10.1103/PhysRevB.82.113106 PACS number(s): 71.36.+c, 78.20.−e

Polaritonic structures could enable a new generation of ultralow power optoelectronic devices such as lasers[1] and optical switches[2] and could serve as a platform for studying Bose-Einstein condensation at room temperature. Polaritonic structures containing exciton-polaritons are formed when excitons in a material are strongly coupled to the vacuum electric field of an optical microcavity. This occurs when the decay rates of the excitons and the cavity mode are slower than the rate of energy exchange between them. Consequently, the system takes on new eigenstates known as exciton-polaritons, and the limit of strong coupling is reached.[3] If a sufficiently high population of polaritons is produced in the cavity, these composite bosonic particles can condense. The emission from the condensate is known as polaritonic lasing, which has been achieved in GaAs (Ref. 4) and CdTe (Ref. 5) quantum wells at cryogenic temperatures, and in bulk GaN (Ref. 1) and GaN/AlGaN quantum wells[6] at room temperature. Recently, the first polariton lasing from an organic material was demonstrated in a single-crystal anthracene microcavity.[7] However, the observed power threshold for lasing in the anthracene microcavity was significantly higher than expected, in part due to exciton-exciton annihilation in the excitonic layer.

A promising material set for achieving low-threshold polariton lasing in organic materials is J-aggregated molecular thin films. Previous work has demonstrated strong coupling in J-aggregate microcavities,[8,9] as well as polariton electroluminescence[10] and ultrafast relaxation between polariton branches.[11] However, J-aggregate polariton lasing remains elusive. In this paper we study exciton dynamics in highly absorbing J-aggregated organic films in polariton microcavities.[12] We show that the J-aggregate excitonic material exhibits significant exciton-exciton annihilation, which competes with the build up of a threshold polariton population necessary for lasing action. The annihilation process is attributed to the large incoherent diffusion radius of excitons in the J-aggregated film.

The J-aggregate material is studied both as an isolated thin film and as the excitonic layer of a polaritonic cavity. The isolated thin film is grown by sequential immersion of a glass substrate in solutions of the J-aggregating cyanine dye 5,6-dichloro-2-[3-[5,6-dichloro-1-ethyl-3-(3-sulfopropyl)-2(3H)-benzimidazolidene]-1-propenyl]-1-ethyl-3-(3-sulfopropyl) benzimidazolium hydroxide, inner salt, sodium salt, N. K. Dye Chem, and a solution of polydialylldimethylammonium chloride following Bradley *et al.*[13] This layer-by-layer growth produces a (5.1 ± 0.1) nm thick films with an absorption linewidth of 46 meV (13 nm), peaked at the exciton resonant energy of $E_{ex}=2.08$ eV (596 nm), with a peak absorption of $\alpha=10^6$ cm^{-1}.

The microcavity samples [Fig. 1(a)] are formed by sputter depositing a 4.5 pair distributed Bragg reflector (DBR) on a quartz substrate, followed by a $\lambda/4n$ SiO_2 spacer layer, where n is the index of refraction and $\lambda=596$ nm. The J-aggregate film is then deposited, followed by a 100 nm thick spin-coated layer of polyvinyl alcohol (PVA, 99.8% hydrolyzed, Sigma Aldrich). The PVA layer acts as the top spacer layer of the cavity and enhances the photoluminescence (PL) external quantum yield of the film from 7% to 42%. A thermally evaporated TAZ [3-(biphenyl-4-yl)-4-phenyl-5-(4-tert-butylphenyl)-1,2,4-triazole] layer forms the remainder of the cavity spacer. The structure is capped with a 300 nm thick thermally evaporated silver mirror, resulting in a cavity Q of 60 [Fig. 1(a)]. The total thickness of the cavity region is tuned by varying the thickness of the TAZ layer, thereby changing the detuning between the J-aggregate exciton ($E_{ex}=2.08$ eV) and the cavity mode.

Figure 1(b) shows the mode splitting observed in the reflectivity of devices with different cavity-exciton detunings. The peak energy of the lower polariton branch PL is observed to follow the lower polariton reflectivity [Fig. 1(c)], indicating that the observed emission originates from the decay of polaritons. The reflectivity and PL data are collected at normal incidence to the cavity. The polaritonic dispersion relation for these devices is shown in Fig. 1(d), demonstrating characteristic polaritonic anticrossing at zero detuning with a Rabi splitting of 160 meV.

The polariton dynamics are investigated by pumping the cavities nonresonantly with TM polarized light at $\lambda=532$ nm through the DBR at 60° relative to normal. The polariton PL is collected at normal incidence to the sample and imaged on a charge coupled device (CCD) spectrometer.

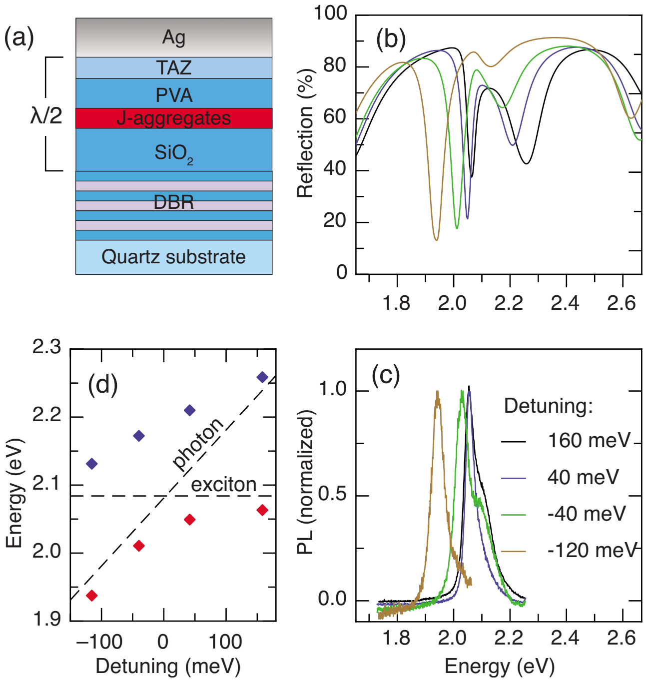

FIG. 1. (Color online) (a) DBR-metal microcavity with a J-aggregate excitonic layer and a total optical path length of λ/2 where λ=596 nm. (b) The reflectivity of devices having different cavity-exciton detunings achieved by varying the TAZ thickness. (c) The corresponding photoluminescence. (d) Energies of the upper and lower polaritons as a function of exciton-cavity detuning extracted from the reflection plots of part (b). The bare exciton and cavity dispersions are shown as dashed lines.

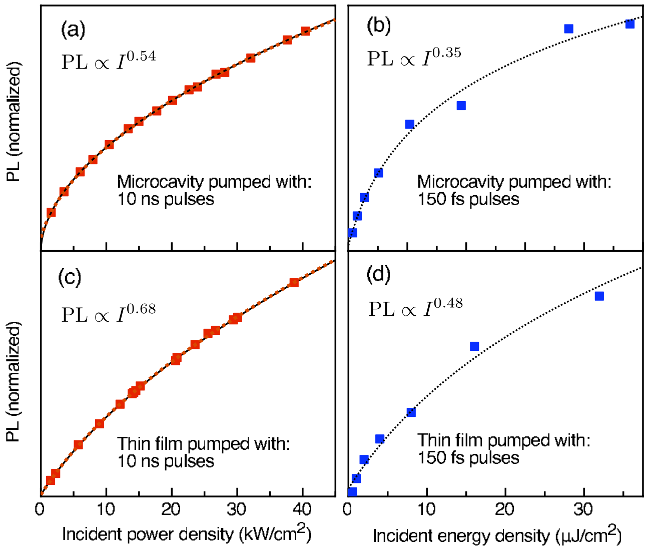

FIG. 2. (Color online) PL intensity dependence for: a microcavity pumped with λ=532 nm (a) 10 ns pulses and (b) 150 fs pulses; and a J-aggregate thin film pumped with (c) 10 ns pulses and (d) 150 fs pulses. The solid lines are fits to Eq. (2) [parts (a) and (c)] while dashed lines are fits to a power law. Fits overlap in parts (a) and (c).

To fully characterize the behavior of the devices in a wide range of excitation power regimes, three pump sources are utilized: a continuous wave (cw) laser at λ=532 nm, a 10 ns pulsed laser at λ=532 nm (10 Hz repetition rate), and a 150 fs pulsed laser at λ=532 nm (1 kHz repetition rate). With cw excitation, the devices show a linear increase in PL intensity with increasing excitation power. With 10 ns excitation pulses, the PL begins to show a sublinear power-law dependence ($\mathrm{PL} \propto I^{0.54}$) as a function of the pump intensity, with the effect becoming more pronounced with 150 fs excitation pulses ($\mathrm{PL} \propto I^{0.35}$) [Figs. 2(a) and 2(b)]. Devices with a range of cavity-exciton tunings as well as cavities with higher Q of 115 were tested and all show qualitatively similar sublinear behavior.

To elucidate the role of the microcavity versus the excitonic layer in the sublinear PL dependence, we tested J-aggregate thin films grown on glass substrates (i.e., the active layer without the cavity). A similar, but less pronounced, sublinear dependence is observed for the thin film ($\mathrm{PL} \propto I^{0.68}$ with 10 ns excitation and $\mathrm{PL} \propto I^{0.48}$ with 150 fs excitation), indicating that the excitonic component of the device is responsible for the sublinear response of the microcavity [Figs. 2(c) and 2(d)]. We rule out the sublinear power dependence as being due to absorption saturation, as only 1% of the molecules are excited at the highest powers. Furthermore, the films show no PL or absorption degradation under 10 ns excitation (4 mW/cm^2 maximum average power density) and only slight degradation under 150 fs excitation (40 mW/cm^2 maximum average power density) that is insufficient to account for the sharp roll off in PL quantum yield.

The sublinear behavior of the J-aggregate thin films and the microcavities is well modeled by exciton-exciton annihilation, a process in which excitons at high densities can be nonradiatively destroyed via exciton-exciton interactions.[14–16] The kinetics of excitons in organic materials are modeled by the two-body rate equation

$$\frac{\partial n}{\partial t} = -\Gamma n - \frac{1}{2}\gamma n^2 + I_{in}\sigma n_{mol}, \qquad (1)$$

where n is the exciton density in cm^{-3}, σ is the absorption cross section at the pump wavelength in cm^2, I_{in} is the pump intensity in photons/cm^2, Γ is the single exciton decay rate (radiative and nonradiative components), n_{mol} is the three-dimensional density of dye molecules in cm^{-3}, and γ is the annihilation rate constant in cm^3/s. Under 10 ns pulsed excitation the material can be considered in quasisteady state ($\tau_{pulse} \gg 1/\Gamma$) and the solution to Eq. (1) is

$$n = \frac{\Gamma}{\gamma}\left(\sqrt{1 + \frac{2\gamma\sigma n_{mol}}{\Gamma^2} I_{in}} - 1\right). \qquad (2)$$

The observed power dependence shows a good fit to Eq. (2) [Figs. 2(a) and 2(c)], suggesting that exciton-exciton annihilation is present in the excitonic material. The absorption cross section of a single dye molecule at λ=532 nm is found to be $\sigma = 6.25 \times 10^{-17}$ cm^{-2} and the in-plane density is $n_{mol} = 1 \times 10^{15}$ cm^{-2} given a 5 nm film thickness and a molecular density[13] of 2 nm^{-3}. The single exciton decay rate is determined from time-resolved PL measurements to be 45 ps. Based on the fit of Eq. (2), the annihilation rate constant is $\gamma = 5.2\times10^{-6}$ cm^3/s in the microcavity and $\gamma = 1.1\times10^{-6}$ cm^3/s in the isolated J-aggregate thin film.

The annihilation rate constant can be related to the exciton diffusion constant D using[17]

$$\gamma = 4\pi D R_c, \tag{3}$$

where R_c is the maximum distance between two excitons at which annihilation occurs. Annihilation of singlet excitons is dominated by dipole-dipole interactions; hence, R_c is approximated to be the Förster radius, which we calculate to be 4 nm in these J-aggregate thin films. If the diffusion in the 5 nm thin film is taken to be two dimensional, then the in-plane diffusion length, in the absence of annihilation, is

$$L = \sqrt{\frac{2D}{\Gamma}}. \tag{4}$$

For the quasisteady state excitation of the isolated thin films, we find $L_{TF} = 44$ nm, which is substantially longer than the <20 nm diffusion lengths typically found in amorphous organic materials.[18] In the microcavity, the annihilation rate constant is significantly larger than in the thin film, giving a diffusion length of $L_{MC} = 115$ nm in the absence of annihilation. The increased annihilation rate in the cavity is attributed to coupling of the excitons to the cavity mode,[19] which increases the effective diffusion length of the excitons due to absorption and reemission within the cavity (i.e., the oscillatory exchange of energy characteristic of strong coupling).

The time dependence of the exciton population also shows that annihilation is a valid model for exciton dynamics in the film. We investigate the exciton population relaxation by exciting the thin films with 5 ps pulses at $\lambda = 532$ nm at varying incident energy densities (Fig. 3) and collecting the time-dependent PL. The PL is imaged by a streak camera and a CCD spectrometer, having a Gaussian instrument response function (IRF) with a full width at half maximum of 6 ps. In this regime of short pulse excitation ($\tau_{pulse} \ll 1/\Gamma$), the pumping term in Eq. (1) is set to zero, and the solution is

$$I_{out} = \frac{I_{in}}{e^{\Gamma t}\left[1 + \frac{\gamma}{2\Gamma}n(0)\right] - \frac{\gamma}{2\Gamma}n(0)}, \tag{5}$$

where $n(0)$ is the number of excitons per unit volume at $t = 0$. The time-dependent PL fits to a convolution of Eq. (5) with the instrument response function (Fig. 3), which again shows that exciton-exciton annihilation is a valid model for exciton dynamics in the film. Fitted values of γ vary from 3.9×10^{-5} cm^3/s at low-intensity excitation (0.147 μJ/cm^2) to 8.1×10^{-6} cm^3/s at high-intensity excitation (1.30 μJ/cm^2) while the single exciton decay rate is $1/\Gamma = 45$ ps, independent of excitation energy. Using Eqs. (3) and (4) the diffusion length L_{TF} is found to be 245 nm at low-intensity excitation and 135 nm at high-intensity excitation. This incoherent delocalization size is much larger than the coherent size of a J-aggregate exciton which is typically ~16 molecules[15] (radius of 3 nm). The apparent reduction in the annihilation-free diffusion length at higher intensities can be attributed to rapid annihilation of nonrelaxed excitons at times <100 fs after excitation,[20,21] which cannot be resolved with our measurement setup.

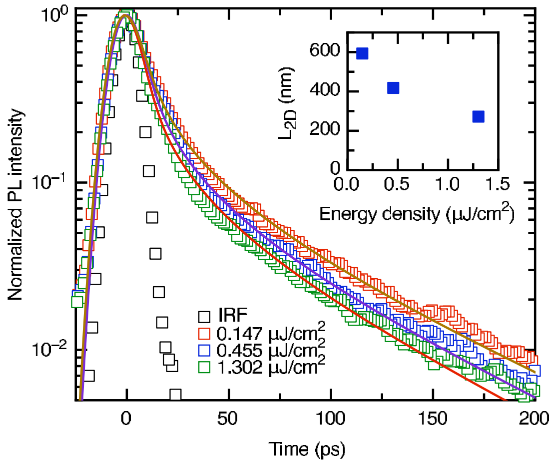

FIG. 3. (Color online) Time-dependent PL at $\lambda = 596$ nm from a J-aggregate thin film excited with 5 ps pulses at $\lambda = 532$ nm with varying energy densities. The data are fit to the convolution of the nonexponential population decay [Eq. (5)] and the IRF. The inset shows the in-plane diffusion length in the absence of annihilation.

The sublinear PL power dependence and the nonexponential PL time dependence support exciton-exciton annihilation as the nonlinear mechanism in the J-aggregate thin film active layer of the microcavities. This result has important implications for achieving polariton lasing using J-aggregate materials. Annihilation processes decrease the exciton lifetime, and hence the polariton lifetime, which increases the polariton lasing threshold density. Furthermore, annihilation competes with polariton-polariton scattering, which is one of the possible mechanisms for populating the $k = 0$ state of the polariton dispersion (the polariton trap).[19,22] Our results show that achieving low-threshold polariton lasing in organic materials will require materials that do not exhibit exciton-exciton annihilation and still possess the necessary properties for strong coupling to a cavity, such as high oscillator strength, narrow linewidth, and small Stokes shift. Alternatively, exciton-exciton interactions can be minimized by either nanopatterning the excitonic layer of the microcavity to reduce the diffusion length or by doping the excitonic material into a wider gap host matrix.

The authors thank Q. Zhang, T. Atay, and A. Nurmikko from Brown University for contributions to the time-resolved experiments. We also thank M. Scott Bradley and Semion Saikin for valuable discussions. This work was funded by the Energy Frontiers Research Center on Excitonics, sponsored by the Department of Energy. G.M.A. acknowledges support from the Hertz Foundation and the National Science Foundation.

*Present address: Institute for Nanotechnology and Advanced Materials, Department of Chemistry, Bar-Ilan University, Ramat Gan 52900, Israel.

[1] S. Christopoulos, G. Baldassarri Höger von Högersthal, A. J. D. Grundy, P. G. Lagoudakis, A. V. Kavokin, J. J. Baumberg, G. Christmann, R. Butté, E. Feltin, J.-F. Carlin, and N. Grandjean, Phys. Rev. Lett. **98**, 126405 (2007).

[2] D. Bajoni, E. Semenova, A. Lemaitre, S. Bouchoule, E. Wertz, P. Senellart, S. Barbay, R. Kuszelewicz, and J. Bloch, Phys. Rev. Lett. **101**, 266402 (2008).

[3] A. Kavokin, G. Malpuech, and B. Gil, MRS Internet J. Nitride Semicond. Res. **8**, 3 (2003).

[4] H. Deng, G. Weihs, C. Santori, J. Bloch, and Y. Yamamoto, Science **298**, 199 (2002).

[5] J. Kasprzak, M. Richard, S. Kundermann, A. Baas, P. Jeambrun, J. M. J. Keeling, F. M. Marchetti, M. H. Szymańska, R. André, J. L. Staehli, V. Savona, P. B. Littlewood, B. Deveaud, and L. S. Dang, Nature (London) **443**, 409 (2006).

[6] G. Christmann, R. Butte, E. Feltin, J. F. Carlin, and N. Grandjean, Appl. Phys. Lett. **93**, 051102 (2008).

[7] S. Kéna-Cohen and S. R. Forrest, Nat. Photonics **4**, 371 (2010).

[8] D. Lidzey, D. Bradley, M. Skolnick, T. Virgili, S. Walker, and D. Whittaker, Nature (London) **395**, 53 (1998).

[9] D. G. Lidzey, D. D. C. Bradley, T. Virgili, A. Armitage, M. S. Skolnick, and S. Walker, Phys. Rev. Lett. **82**, 3316 (1999).

[10] J. R. Tischler, M. S. Bradley, V. Bulovic, J. H. Song, and A. Nurmikko, Phys. Rev. Lett. **95**, 036401 (2005).

[11] D. G. Lidzey, A. M. Fox, M. D. Rahn, M. S. Skolnick, V. M. Agranovich, and S. Walker, Phys. Rev. B **65**, 195312 (2002).

[12] J. R. Tischler, M. S. Bradley, Q. Zhang, T. Atay, A. Nurmikko, and V. Bulovic, Org. Electron. **8**, 94 (2007).

[13] M. Bradley, J. R. Tischler, and V. Bulovic, Adv. Mater. **17**, 1881 (2005).

[14] J. Moll, W. Harrison, D. Brumbaugh, and A. Muenter, J. Phys. Chem. A **104**, 8847 (2000).

[15] M. van Burgel, D. A. Wiersma, and K. Duppen, J. Chem. Phys. **102**, 20 (1995).

[16] C. Swenberg, N. Geacintov, and M. Pope, Biophys. J. **16**, 1447 (1976).

[17] P. E. Shaw, A. Ruseckas, J. Peet, G. C. Bazan, and I. D. W. Samuel, Adv. Funct. Mater. **20**, 155 (2010).

[18] R. R. Lunt, N. C. Giebink, A. A. Belak, J. B. Benziger, and S. R. Forrest, J. Appl. Phys. **105**, 053711 (2009).

[19] M. Litinskaya, Phys. Lett. A **372**, 3898 (2008).

[20] A. Ruseckas, P. Wood, I. D. W. Samuel, G. R. Webster, W. J. Mitchell, P. L. Burn, and V. Sundstrom, Phys. Rev. B **72**, 115214 (2005).

[21] A. J. Lewis, A. Ruseckas, O. P. M. Gaudin, G. R. Webster, P. L. Burn, and I. D. W. Samuel, Org. Electron. **7**, 452 (2006).

[22] M. Litinskaya, P. Reineker, and V. M. Agranovich, Phys. Status Solidi A **201**, 646 (2004).